



OPEN

DATA DESCRIPTOR

QM-symex, update of the QM-sym database with excited state information for 173 kilo molecules

Jiechun Liang¹ , Shuqian Ye¹, Tianshu Dai², Ziyue Zha¹, Yuechen Gao¹ & Xi Zhu¹ 


In the research field of material science, quantum chemistry database plays an indispensable role in determining the structure and properties of new material molecules and in deep learning in this field. A new quantum chemistry database, the QM-sym, has been set up in our previous work. The QM-sym is an open-access database focusing on transition states, energy, and orbital symmetry. In this work, we put forward the QM-symex with 173-kilo molecules. Each organic molecular in the QM-symex combines with the C_n, h symmetry composite and contains the information of the first ten singlet and triplet transitions, including energy, wavelength, orbital symmetry, oscillator strength, and other quasi-molecular properties. QM-symex serves as a benchmark for quantum chemical machine learning models that can be effectively used to train new models of excited states in the quantum chemistry region as well as contribute to further development of the green energy revolution and materials discovery.

Background & Summary

The past few decades have witnessed the construction of various quantum chemical databases such as GDB-13¹, QM7², QM7b³, and QM9⁴. These databases report molecular structure and several energy-related properties, including entropy and band gap. GDB-13 lists 970 million synthetic organic molecules and contains up to 13 heavy atoms, while the QM7 database provides the coulomb matrix and atomization energy of 7165 organic molecules for the GDB-13 subset containing 7 heavy atoms. QM7b extends 13 additional properties of QM7, such as energies of the highest occupied molecular orbital (HOMO) and the lowest unoccupied molecular orbital (LUMO), polarization, and excitation energy of 7,211 organic molecules. Montavon *et al.*⁵ used these databases to train multi-task deep neural networks, using coulomb matrices as descriptors to predict these additional attributes with reasonable accuracy. The most widely used one is the QM9 dataset constructed by Von Lilienfeld *et al.*, which contains up to 9 heavy atoms and has ground state geometry, dipole moment, polarimetry, enthalpy, and free energy of approximately 134k molecules, which is popular in the field of artificial intelligence chemistry (AIC).

The excited-state properties of molecules are of great value in practical applications—for example, photosensitizers, phosphorescent molecular probes, and photodynamic therapy (PDT). However, most current open-access databases fail to provide sufficient information on excited-state properties. The famous QM8^{5,6} contains TD-DFT and CC2 level of electron spectra informations, but some exact transition information such as oscillator strength, transition energy, or transition symmetry is still missing. In recent decades, many discussions and studies on singlet fission have been raised. Singlet fission (SF), with its induced energy conversion process capable of exceeding the traditional Shockley-Queisser limit⁷, enables a singlet exciton to split into two triplet excitons, and is regarded to be capable of improving the efficiency of current photovoltaics. Previous researchers have demonstrated various designs for SF photovoltaics^{8–10}, while the development of appropriate SF materials is hindered by limited SF structure database. By involving excited state information, our quantum chemistry database can reveal the development trend of compound properties and guide the rational design of new materials.

Another vital application of accelerated development is artificial intelligence. Checking the excited-state properties of each molecule experimentally is time and energy consuming, and thus the use of quantum mechanical computation (QM) or machine learning algorithm (ML) is necessary in enabling scholars to study the structure

¹Shenzhen Institute of Artificial Intelligence and Robotics for Society (AIRS), 13-15F, Tower G2, Xinghe World, Rd Yabao, Longgang District, Shenzhen, Guangdong, 518172, China. ²Department of Mathematics, College of Letters and Science, University of California, Santa Barbara 522 University RD, Santa Barbara, CA, 93106-3080, USA.  e-mail: zhuxi@cuhk.edu.cn

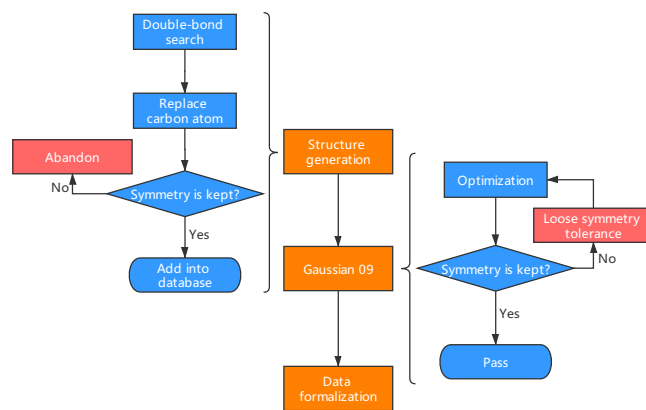


Fig. 1 The overall process of the QM-symex generation. The middle part is the mainstream, the left part shows the process of new molecules generation, and the right part is the validation through Gaussian 09.

and properties of material molecules more efficiently^{11–17} and to compile large databases. However, quantum mechanical computation and machine learning algorithms, especially neural networks, are able to come up with relatively good performance only if large databases are utilized in training and debugging models. To tackle this problem, QM-symex provides an efficient training and evaluation database for data-driven machine learning models in quantum chemistry. Given the information of the first ten singlet states and triplet states, the database has more application value than the original database in terms of the correlation characteristics of orbital symmetry, such as excitation degeneracy and selection rules of transition. This symmetric database can provide additional benefits by allowing researchers to understand and discover structural properties from ML perspectives, eventually make essential contributions to discovering chemical relationships and the synthesis of new organic materials by strong fitting and classification.

What is more, the study of excited molecules is of great importance to the industrialization of renewable resources. Solar energy is one of the essential renewable energy sources and the day-night cycle on earth makes the storage of solar energy an essential prerequisite for solar energy research and utilization. Under the current circumstance, high cost of inorganic materials widely used to store solar energy makes it difficult to realize large-scale commercialization of solar energy. Our research makes it possible to lower the cost of storing solar energy by substituting inorganic materials with the organic ones. In fact, for organic molecules, due to the corresponding relationship between the excited state and the quasi-particle condition, the transition of electrons in different molecular orbitals will lead to many vital phenomena, such as photochromism and fluorescence. More importantly, information on the excited state of the molecule contributes to energy generation. Organic molecules with its low-cost, easy-to-process, and regulated characteristics provide an ideal target for the next generation of the photon industry. So far, much work has focused on the discovery of excited states and corresponding data¹⁸, including the study of organic photoelectric sensing materials and the study of excited states and photochemistry of organic molecules.

Methods

In this work, we propose a quantum chemical symmetric excited state database (QM-symex)¹⁹ that contains 173k molecules. Each organic molecule in QM-symex has been combined with C_n, h symmetry composites²⁰. Each molecule in QM-symex contains information about the first ten Singlet transitions and Triplet transitions, including energy, wavelength, symmetry, oscillator strength, spin, and other excimer properties.

To prepare the database for better machine learning performance, another 38k molecule is generated in addition to the 135k molecules from QM-sym. We do not use double-bonded carbon atoms at the center in new molecules to ensure the stability. Initially, we decide which symmetry to be used, generate an initial carbon chain, and choose whether to lengthen the side chain or replace the hydrogen atom with halogens. This lengthening and replacement process are also forced to keep the original symmetry. The optimization is performed with 100 cycles to guarantee the minimum energy and stable position. To check whether the molecule still has the original symmetry after optimization, we use a validation step in the Gaussian09 for each cycle. When the position of atoms reaches the restrictions, we will lose the symmetry tolerance and check whether the symmetry is kept overall. If the symmetry is broke, this molecule will be abandoned. For the whole 173k molecules, we choose $Nstates = 10$ and keep the B3LYP/6-31 G level of theory with $Symm = VeryLoose$ to calculate the first ten transition states. The overall process of database generalization is shown in Fig. 1.

All the excited state information is extracted from the output from Gaussian09, and is collect into correlated xyz file. Now the QM-symex database is publicly available on figshare (see the code availability section below). It now includes 173k molecular structures (QM_symex_i.xyz) and all properties information in QM-sym, and we add the information of the first ten singlet and triplet transition, including energy, wavelength, orbital symmetry, transition distance, and other quasi-molecular properties. Details about the available properties are recorded in the README file and Table 1 below. Figure 2 shows the overall composition of QM-symex. With 38k new molecules, the C_2, h occupies 46% capacity and C_3, h , C_4, h occupy 41% and 13%, and most of the molecules have three to nine states in the first transition, as shown in Fig. 2.

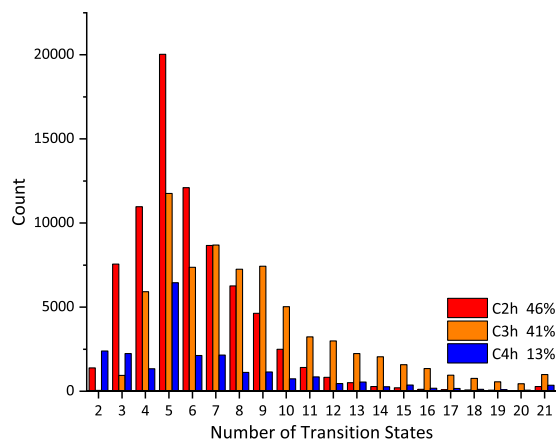


Fig. 2 Number of states in the first transition. All of the molecules are included. The legend shows the symmetry component of QM-symex. The lower scheme is the number of transition states versus the count of molecules. Most of the molecules have less than ten states inside the first transition. The colors of both diagrams have the same meaning. Red, orange and blue colors denote C_2h , C_3h , and C_4h molecules.

No.	Property	Unit	Description
1	TS	/	Transition symmetry group
2	E_t	eV	Transition energy
3	λ	nm	Wavelength
4	f	/	Oscillator strength
5	S^2	/	Spin

Table 1. Properties from Gaussian09 calculation. The previous properties from Qm-sym were not listed here. This table shows the properties below xyz coordinates.

Line	Content
1, 3 + $N \cdot n_a$	Original QM-sym data (properties and xyz coordinates)
4 + $N \cdot n_a$	Position of HOMO
5 + $N \cdot n_a$	Information of the first Singlet/Triplet transition
...	...
14 + $N \cdot n_a$	Information of the tenth Singlet/Triplet transition

Table 2. xyz file formats for molecular structure and properties. The first to the 3 + $N \cdot n_a$ lines have the same format as QM-sym. Started from 4 + $N \cdot n_a$ are the lines for excited states information. The detailed format is discussed above in the main body.

Data Records

All the xyz file is contained in a package on figshare¹⁹. The xyz file contains the atomic coordinates and the prediction attribute information from the Gaussian 09 calculation; Each structure is indexed as QM_symex_i.xyz, where i is the index of the ordered structure in the database. The xyz file format is one of the most widely used file formats in molecular chemistry, and the structure can be visualized using many free software programs like VESTA. Table 2 presents the basic outline of the xyz format. N is the symmetry of the molecule C_Nh , and n_a is the number of atoms in each symmetry unit. The format of the first 3 + $N \cdot n_a$ lines is the same as QM-sym with the same ID. Starting from the 4 + $N \cdot n_a$ is the transition information. The 4 + $N \cdot n_a$ line shows the position of HOMO, for instance, “71”. The following ten lines are the ten transitions. In each line, the information is shown in two-part. The first part is the Singlet transitions and followed by Triplet transitions. The format is: “transition number | (Singlet Part) transition symmetry, energy (eV), wavelength (nm), oscillator strength, spin | (first state) origin orbital, target orbital, probability | (second state) ... | (Triplet part) transition symmetry, energy (eV), wavelength (nm), spin | (first state) origin orbital, target orbital, probability | (second state) ...”. Take an example as follows: “4|EU 3.9319 315.33 0.0045 0.000|338 341 0.70100|EG 3.8932 318.46 0.0000 2.000|335 344 -0.13252|335 345 -0.12772|340 342 0.59427|340 343 0.21201” from QM_symex_210542.xyz. “4” means it is the fourth transition. “EU,” “EG” are the symmetry of Singlet and Triplet transition. “3.9319” and “3.8932” are the energy of both transitions in eV. “315.33” and “318.46” are wavelengths in nm. “0.0045” and “0.0000” are oscillator strengths, and the following “0.000” and “2.000” are the spin. The next blocks show all the transition states. In this example, the fourth Singlet transition has only one state, and the fourth Triplet transition has four states.

Reference	MAE	maxAE	RMSE
CBS-QB3	4.9 (4.5)	6.9 (5.5)	15.4 (13.4)
G4	5.6 (4.9)	6.6 (5.9)	16.4 (14.4)
G4MP2	6.4 (5.0)	8.0 (6.1)	17.6 (16.0)

Table 3. Benchmark comparison of atomization enthalpies. The data inside the parenthesis are data from QM9, and the other one is the difference comparing to calculated data under B3LYP/6-31 G(2df,p) level.

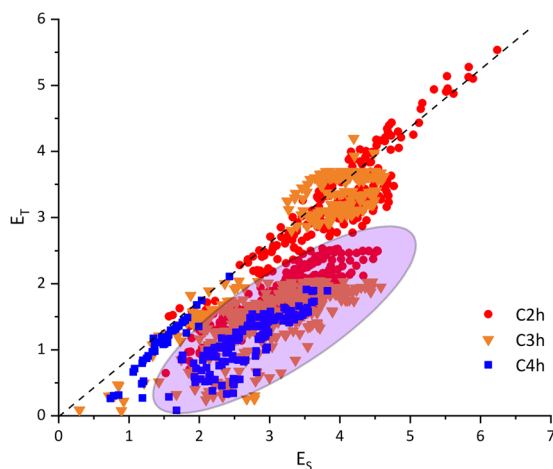


Fig. 3 Singlet transition energy versus Triplet transition energy of random-selected molecules. The red dot, orange triangle, and blue square denote molecules with C_2h , C_3h , and C_4h symmetry. From these molecules, we can see two tendencies. The black dash line denotes the first one, which is $E_S \cong E_T$. The second one is denoted by the purple oval, which is $E_S \cong 2E_T$ and accords with SF condition.

“338 341 0.70100” means that this state is from the 338th orbital to the 341st orbital with a probability of 0.701. It is not a problem to determine the correlation between the number-denoted orbitals because the position of HOMO will be denoted in a previous line, as shown in Table 2. That line tells that the number of HOMO is 340, so this transition is from HOMO-2 to LUMO. The format information is also available in the README file.

Technical Validation

The properties recorded in this database are numerically derived from the DFT calculation and TD-DFT calculation after optimization of molecules with symmetry tolerance and 10^{-5} eV energy convergence. The detailed properties are listed in Table 1. These new molecules are first calculated with B3LYP/6-31 G(2df,p) level in Gaussian 09²¹, and strictly follow the geometry check²⁰. The benchmark with the G4²², G4MP2²³, and CBS-QB3²⁴ is also processed and is shown in Table 3. Inside the parenthesis are the data recorded in the QM9 database. The maximum number of heavy atoms for molecules in QM9 is 9, but in QM-symex, the number of heavy atoms can reach 60, so a slightly larger error in benchmarks is reasonable and tolerable.

Based on a simple Molecular orbital picture²⁵, the energy difference between singlet and triplet excited states depends on the exchange integral of HOMO and LUMO, which can be characterized by the wave function distance. The exchange integral will nearly vanish if the distance between HOMO and LUMO wave function is demonstrated to be significant. As a result, the singlet and triplet excited state will have equal excitation energy, which implies the first tendency $E_S \cong E_T$ in Fig. 3. This can also be verified through the calculation of oscillator strength. For structures satisfying $E_S \cong E_T$, the singlet oscillator strength tends to approach zero value even if it is symmetry allowed. The second tendency acts as a boundary to distinguish potential SF structures and is rounded by a purple oval in Fig. 3. These molecules satisfy $E_S \cong 2E_T$ and have a large amount, which is helpful to SF-correlated research, and corresponding AI approaches.

For the structure in Fig. 4, we show an example of singlet and triplet transitions on the same molecule. The degeneracy of HOMO is 2, so the two orbitals in the lower half can be considered the same due to the same symmetry. The enormous probabilities of the first Singlet transition and Triplet transition are from HOMO to LUMO and from HOMO to LUMO + 2, which are 0.61 and 0.48, as shown in the middle part. The symmetry, energy, wavelength, oscillator strength, and spin of these two transitions are also shown in the lower part of Fig. 4. As is shown in the spin density cloud, the wavefunction of HOMO mainly focuses on the benzene ring, while the wavefunction of LUMO is localized around the halogen atom, resulting in a low exchange integral. Thus, the oscillator strength for singlet excited state is small, and the singlet excited energy is merely larger than triplet excited energy. The triplet excited state is classically forbidden; hence the oscillator strength for triplet is precisely zero.

Nowadays, neural network method can predict the quantum chemical properties with high accuracy; the deep learning community desires a new baseline to evaluate the performance of their method. As far as we know, QM-symex is the first database to provide excited-state data with symmetrical molecules, together with other

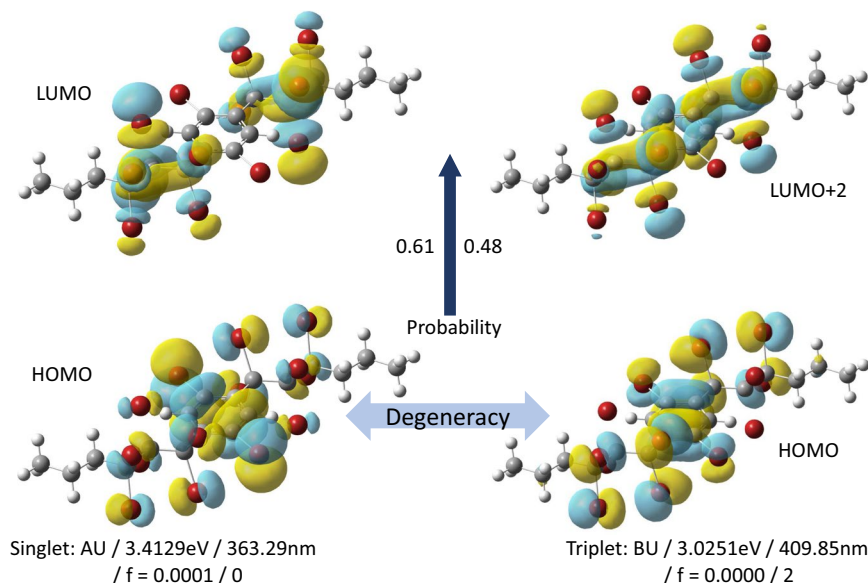


Fig. 4 Example of the first transition of QM-symex No.001550. The left part is the Singlet transition, and the right part is the Triplet transition. The symmetry, energy, wavelength, oscillator strength, and S^2 of Singlet transition are AU, 3.4129 eV, 363.29 nm, 0.0001, and 0. For Triplet transition, they become BU, 3.0251 eV, 409.85 nm, 0, and 2. The Singlet transition is from the HOMO to LUMO, and the Triplet transition is from the HOMO (degeneracy = 2) to the LUMO + 2. On either hand of the middle upward arrow are two probabilities for Singlet transition state (0.61) and Triplet transition state (0.48). Here 0.61 and 0.48 are the highest probabilities over the Singlet and Triplet states.

Orbital	LUMO	LUMO +1	LUMO +2	LUMO +3	LUMO +4	LUMO +5
CE	2.50%	8.38%	9.63%	12.66%	18.71%	22.76%
Orbital	HOMO	HOMO -1	HOMO -2	HOMO -3	HOMO -4	HOMO -5
CE	2.59%	7.90%	15.95%	24.04%	27.97%	29.20%

Table 4. The prediction classification error (CE) for vibration symmetry on different orbits.

properties, such as energy, heat capacity, and band gap, in both K and R spaces. Compared with the most widely used QM database QM9, QM-symex raises a higher requirement for the method. The number of data needed to be predicted is not fixed but depends on the number of orbits in different molecules. The neural networks should be capable to output different results according to the input molecules. With the excited-states data provided by QM-symex, researchers can encode the correlation between orbital information and quantum chemical properties in their methods to enhance the accuracy in both excited state and quantum chemical properties prediction.

To demonstrate the potential of deep learning method in predicting excited state, we have run SY-GNN²⁶ on this database; the overall classification error for symmetry prediction is 17.01%, and the detailed data are shown in Table 4. The mean-absolute-error (MAE) for vibration frequency prediction is 12.03, and the root-mean-square error (RMSE) 11.81. For vibration mass prediction, MAE is 2.63, RMSE is 4.46. We can see that the accuracy of LUMO classification and HOMO classification are the highest in the conduction band and valence band. Classification accuracy of the neural network drops with the energy difference from HOMO and LUMO. The deep learning method can easily predict the low orbit, but reveals difficulty in explaining high orbit behaviors. This result shows that the calculation and prediction of the error inside the neural network favor the low-energy transition, which is consistent with the theory. The lower accuracy from the orbitals away from HOMO and LUMO shows that further analysis is needed in the neural network to reach higher accuracy on orbital property predictions.

Code availability

The newest version of QM-symex is available on figshare (<https://doi.org/10.6084/m9.figshare.12815276>).

Received: 1 September 2020; Accepted: 27 October 2020;

Published online: 18 November 2020

References

- Blum, L. C. & Raymond, J.-L. 970 million druglike small molecules for virtual screening in the chemical universe database GDB-13. *Journal of the American Chemical Society* **131**, 8732–8733 (2009).
- Rupp, M., Tkatchenko, A., Müller, K.-R. & Von Lilienfeld, O. A. Fast and accurate modeling of molecular atomization energies with machine learning. *Physical review letters* **108**, 058301 (2012).

3. Montavon, G. *et al.* Machine learning of molecular electronic properties in chemical compound space. *New Journal of Physics* **15**, 095003 (2013).
4. Ramakrishnan, R., Dral, P. O., Rupp, M. & Von Lilienfeld, O. A. Quantum chemistry structures and properties of 134 kilo molecules. *Scientific data* **1**, 1–7 (2014).
5. Ruddigkeit, L., Van Deursen, R., Blum, L. C. & Reymond, J.-L. Enumeration of 166 billion organic small molecules in the chemical universe database GDB-17. *Journal of chemical information and modeling* **52**, 2864–2875 (2012).
6. Ramakrishnan, R., Hartmann, M., Tapavicza, E. & Von Lilienfeld, O. A. Electronic spectra from TDDFT and machine learning in chemical space. *The Journal of chemical physics* **143**, 084111 (2015).
7. Smith, M. B. & Michl, J. Singlet fission. *Chemical reviews* **110**, 6891–6936 (2010).
8. Congreve, D. N. *et al.* External quantum efficiency above 100% in a singlet-exciton-fission-based organic photovoltaic cell. *Science* **340**, 334–337 (2013).
9. Yang, L. *et al.* Solution-processable singlet fission photovoltaic devices. *Nano letters* **15**, 354–358 (2015).
10. Jadhav, P. J. *et al.* Triplet exciton dissociation in singlet exciton fission photovoltaics. *Advanced materials* **24**, 6169–6174 (2012).
11. Butler, K. T., Davies, D. W., Cartwright, H., Isayev, O. & Walsh, A. Machine learning for molecular and materials science. *Nature* **559**, 547 (2018).
12. Fernandez, M., Boyd, P. G., Daff, T. D., Aghaji, M. Z. & Woo, T. K. Rapid and accurate machine learning recognition of high performing metal organic frameworks for CO₂ capture. *The journal of physical chemistry letters* **5**, 3056–3060 (2014).
13. Huang, Y. *et al.* Band gap and band alignment prediction of nitride-based semiconductors using machine learning. *Journal of Materials Chemistry C* **7**, 3238–3245 (2019).
14. Takahashi, K. & Takahashi, L. Creating Machine Learning-Driven Material Recipes Based on Crystal Structure. *The journal of physical chemistry letters* **10**, 283–288 (2019).
15. Zhang, Y. & Ling, C. A strategy to apply machine learning to small datasets in materials science. *Npj Computational Materials* **4**, 25 (2018).
16. Zhuo, Y., Mansouri Tehrani, A. & Brgoch, J. Predicting the band gaps of inorganic solids by machine learning. *The journal of physical chemistry letters* **9**, 1668–1673 (2018).
17. Liang, J. & Zhu, X. Phillips-Inspired Machine Learning for Band Gap and Exciton Binding Energy Prediction. *The journal of physical chemistry letters* **10**, 5640–5646 (2019).
18. Abreha, B. G., Agarwal, S., Foster, I., Blaiszik, B. & Lopez, S. A. Virtual Excited State Reference for the Discovery of Electronic Materials Database: An Open-Access Resource for Ground and Excited State Properties of Organic Molecules. *The Journal of Physical Chemistry Letters* **10**, 6835–6841 (2019).
19. Liang, J. *et al.* Qm-symex database. *figshare* <https://doi.org/10.6084/m9.figshare.12815276> (2020).
20. Liang, J., Xu, Y., Liu, R. & Zhu, X. QM-sym, a symmetrized quantum chemistry database of 135 kilo molecules. *Scientific Data* **6**, 1–8 (2019).
21. Frisch, M. *et al.* gaussian 09, Revision d. 01, Gaussian, Inc., Wallingford CT **201** (2009).
22. Curtiss, L. A., Redfern, P. C. & Raghavachari, K. Gaussian-4 theory. *The Journal of chemical physics* **126**, 084108 (2007).
23. Curtiss, L. A., Redfern, P. C. & Raghavachari, K. Gaussian-4 theory using reduced order perturbation theory. *The Journal of chemical physics* **127**, 124105 (2007).
24. Montgomery, J. A. Jr, Frisch, M. J., Ochterski, J. W. & Petersson, G. A. A complete basis set model chemistry. VII. Use of the minimum population localization method. *The Journal of Chemical Physics* **112**, 6532–6542 (2000).
25. Michl, J. & Thulstrup, E. W. Why is azulene blue and anthracene white? A simple MO picture. *Tetrahedron* **32**, 205–209 (1976).
26. Ye, S., Liang, J., Liu, R. & Zhu, X. Symmetrical Graph Neural Network for Quantum Chemistry with Dual Real and Momenta Space. *The Journal of Physical Chemistry A* **124**, 6945–6953 (2020).

Acknowledgements

This work is supported by the Shenzhen Fundamental Research Foundation (JCYJ20180508162801893) and National Natural Science Foundation of China (grant no. 21805234, 22075240). Funding from Shenzhen Institute of Artificial Intelligence and Robotics for Society (AIRS) is appreciated.

Author contributions

All authors designed and performed the research and wrote the paper.

Competing interests

The authors declare no competing interests.

Additional information

Correspondence and requests for materials should be addressed to X.Z.

Reprints and permissions information is available at www.nature.com/reprints.

Publisher's note Springer Nature remains neutral with regard to jurisdictional claims in published maps and institutional affiliations.



Open Access This article is licensed under a Creative Commons Attribution 4.0 International License, which permits use, sharing, adaptation, distribution and reproduction in any medium or format, as long as you give appropriate credit to the original author(s) and the source, provide a link to the Creative Commons license, and indicate if changes were made. The images or other third party material in this article are included in the article's Creative Commons license, unless indicated otherwise in a credit line to the material. If material is not included in the article's Creative Commons license and your intended use is not permitted by statutory regulation or exceeds the permitted use, you will need to obtain permission directly from the copyright holder. To view a copy of this license, visit <http://creativecommons.org/licenses/by/4.0/>.

The Creative Commons Public Domain Dedication waiver <http://creativecommons.org/publicdomain/zero/1.0/> applies to the metadata files associated with this article.

© The Author(s) 2020